Supplementary material for "Contrasted trends in phytoplankton diversity, size structure and carbon burial efficiency in the NW Mediterranean Sea under shifting environmental conditions"

Camille Godbillot[1], Baptiste Pesenti[1], Karine Leblanc[2], Luc Beaufort[1], Cristele Chevalier[2], Julien Di Pane[2], Xavier Durrieu de Madron[3], Thibault de Garidel-Thoron[1]

[1]Aix-Marseille Univ, CNRS, IRD, INRAE, CEREGE, ITEM – Aix-en-Provence, France

[2]Aix-Marseille Univ, Université de Toulon, CNRS, IRD, MIO – Marseille, France

[3]CEFREM, CNRS, Université de Perpignan Via Domitia – Perpignan, France

Contents of the supplementary material

I. Methods

1. *Deriving $CaCO_3$ fluxes and coccolith-$CaCO_3$ fluxes to the traps*

Due to their birefringent nature, it is possible to derive the average thickness of each calcite crystal identified on a microscope image from the average mean gray level of the particle. In turn, with the area of the particle, it is possible to derive a mass of $CaCO_3$ for each crystal, making it possible to determine the total $CaCO_3$ flux to the sediment trap (including the calcite fluxes from non-coccolith particles like foraminifera test fragments etc.), and the coccolith-specific $CaCO_3$ flux. Similar to the particle fluxes, the carbonate fluxes C_i for each source of calcite (coccolith, or other) is calculated as:

$$C_i = \frac{\sum(m_{CaCO3})_i \times A_{slide} \times m_{trap}}{N_{image} \times A_{image} \times m_{sample} \times \Delta_t \times A_{trap}}$$

Where $\sum(m_{CaCO3})_i$ is the sum of the mass of individuals for each source in picograms where m_{CaCO3} is defined as:

$$m_{CaCO3} = \rho_{CaCO3} * A * b * GL * \frac{d_{max}}{GL_{max}}$$

Where ρ_{CaCO3} is the density of calcite (2.71 g/cm^3), A the area in pixels of the particle considered, b the number of square micrometers per pixel (0.0036 in our case), GL the mean grey level of the particle, d_{max} the maximum thickness of the particle (which depends on the camera type and filter applied (Beaufort et al., 2020)), and GL_{max} the maximum gray level. (255 in our case).

2. *Deriving coccolithophore fluxes and relative contributions from coccolith counts*

We used coccolith counts per coccosphere as reported by (Yang & Wei, 2003) to derive coccolithophore counts from coccolith data :

Table S1: Values for coccoliths per coccosphere used in the PCA computation

Species	Coccoliths/Coccospheres	Source
C_Calcidiscus	35	Yang & Wei 2003 C. leptoporus
C_Calcisolenia	120	Yang & Wei 2003, C. murrayi
C_Ehuxleyi	25	Yang & Wei 2003, E huxleyi
C_Florisphaera	124	Yang & Wei 2003, F profunda va profunda
C_Gladiolithus	71	Yang & Wei 2003, G gladiolithus
C_Goceanica	27	Yang & Wei 2003, G oceanica
C_Gspp	16	Yang & Wei 2003, G ericsonii (same muellare)
C_Helicosphaera	29	Yang & Wei 2003, H carteri
C_Pontosphaera	16	Yang & Wei 2003, Japonica
C_Scyphosphaera	10	Yang & Wei 2003, Scyphosphaera apsteinii lopadolith
C_Syracosphaera	39	Yang & Wei 2003, Syracosphaera pulchra
C_Umbellosphaera	20	Yang & Wei 2003, U tenuis
C_Umbilicosphaera	120	Yang & Wei 2003, U sibogae var sibogae

3. *Models*

Confusion matrix for the siliceous material studied:

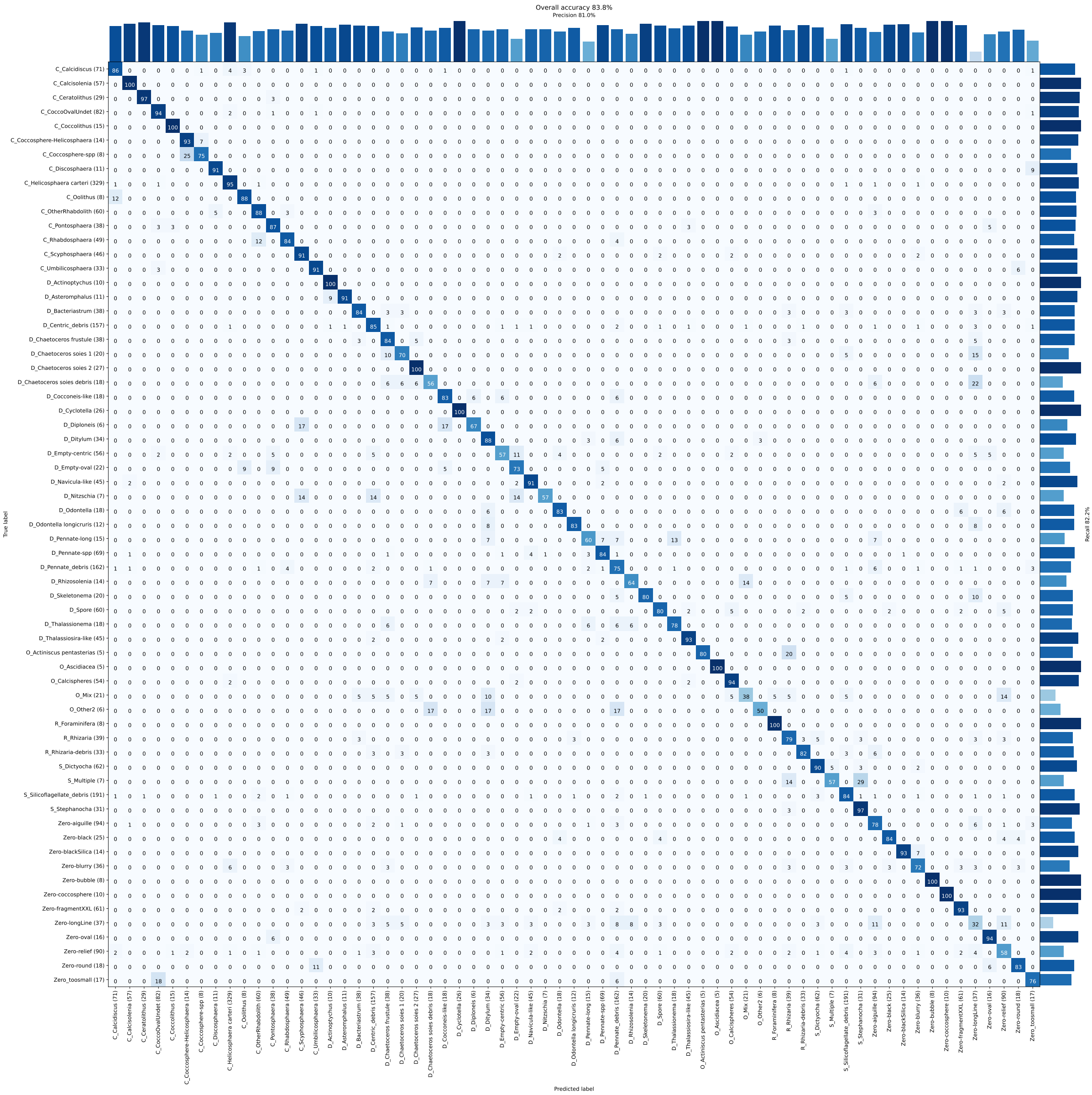

Figure S1 – Confusion matrix obtained from the classification CNN trained on cropped images of the brightfield microscopy protocol.

4. *Environmental parameters*

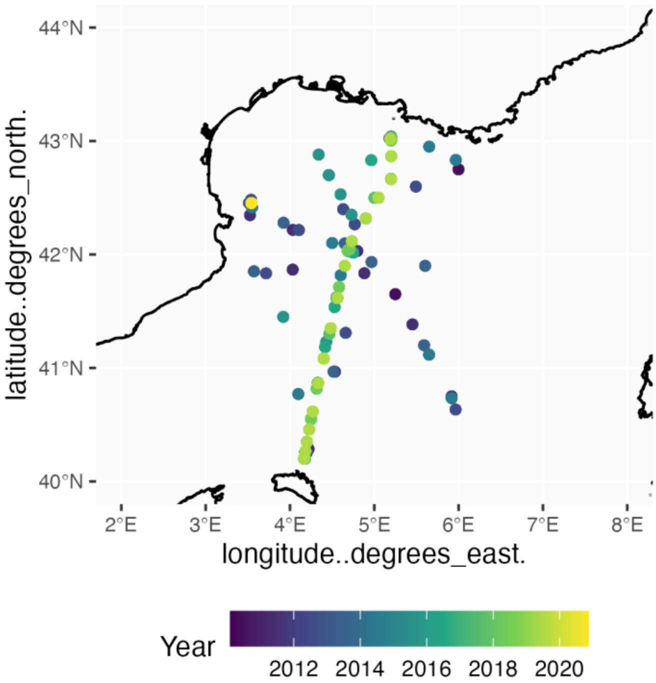

a. Environmental data for the Lionceau sediment trap (Gulf of Lion)

Figure S2 – Location of the different sampling locations of the MOOSE cruises since 2011

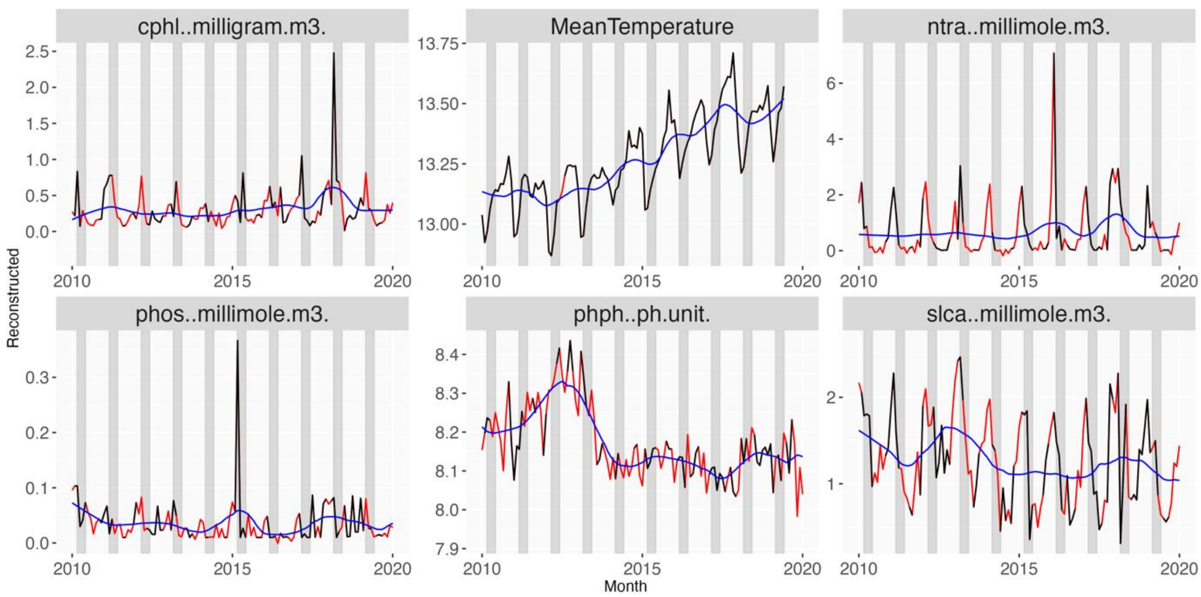

used in this analysis (see Main Text and references therein).

Figure S3 – Monthly averages for the environmental variables considered for the period of study. Mean temperature values are extracted from the Billion probe installed at the Lion site. Other variables are taken from the MOOSE water samples (see Main Text and references therein). Black points: available data. Red: Reconstructed points from the stlplus package. Blue line: trends extracted from the stlplus package.

b. Environmental data for the DYFAMED sediment trap (Ligurian Sea)

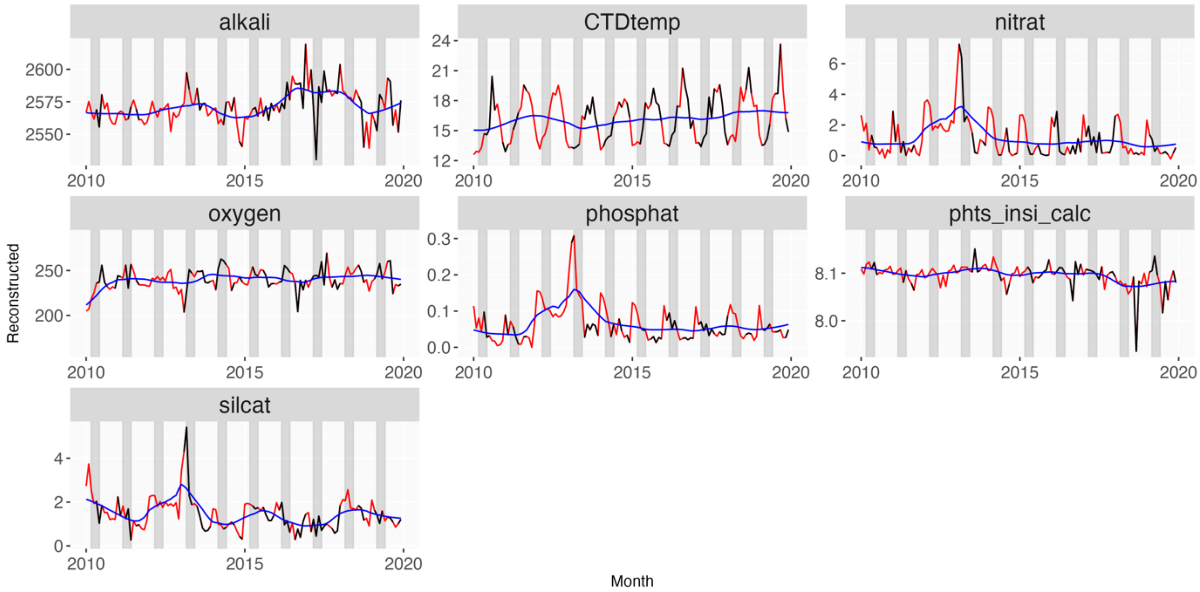

Figure S4 – DYFAMED – interannual variations for the different environmental parameters studied above 50m. The data is extracted from the measurements made on the Niskin bottles during monthly cruises to the site (see Main Text and references therein). Black data points are the original data, red points are the reconstructed variables using stlplus, and the blue line is the trend extracted from the stlplus analysis.

II. Results

1. Validation of count data using the species common in both datasets: helicosphaera carteri

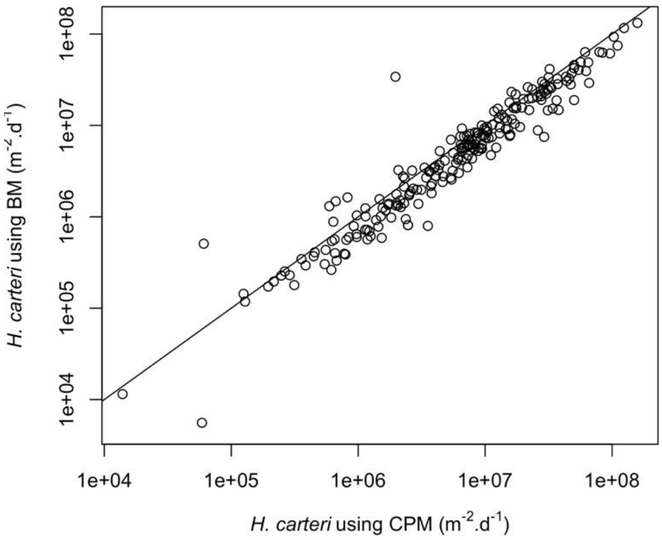

Figure S5 – Scatter plot for the fluxes of the microfossil *Helicosphera carteri* obtained using the image analysis protocol of cross-polarized light images and using the protocol of images taken using brightfield microscopy. This is the DYFAMED example.

2. *Interannual particle and carbon fluxes*

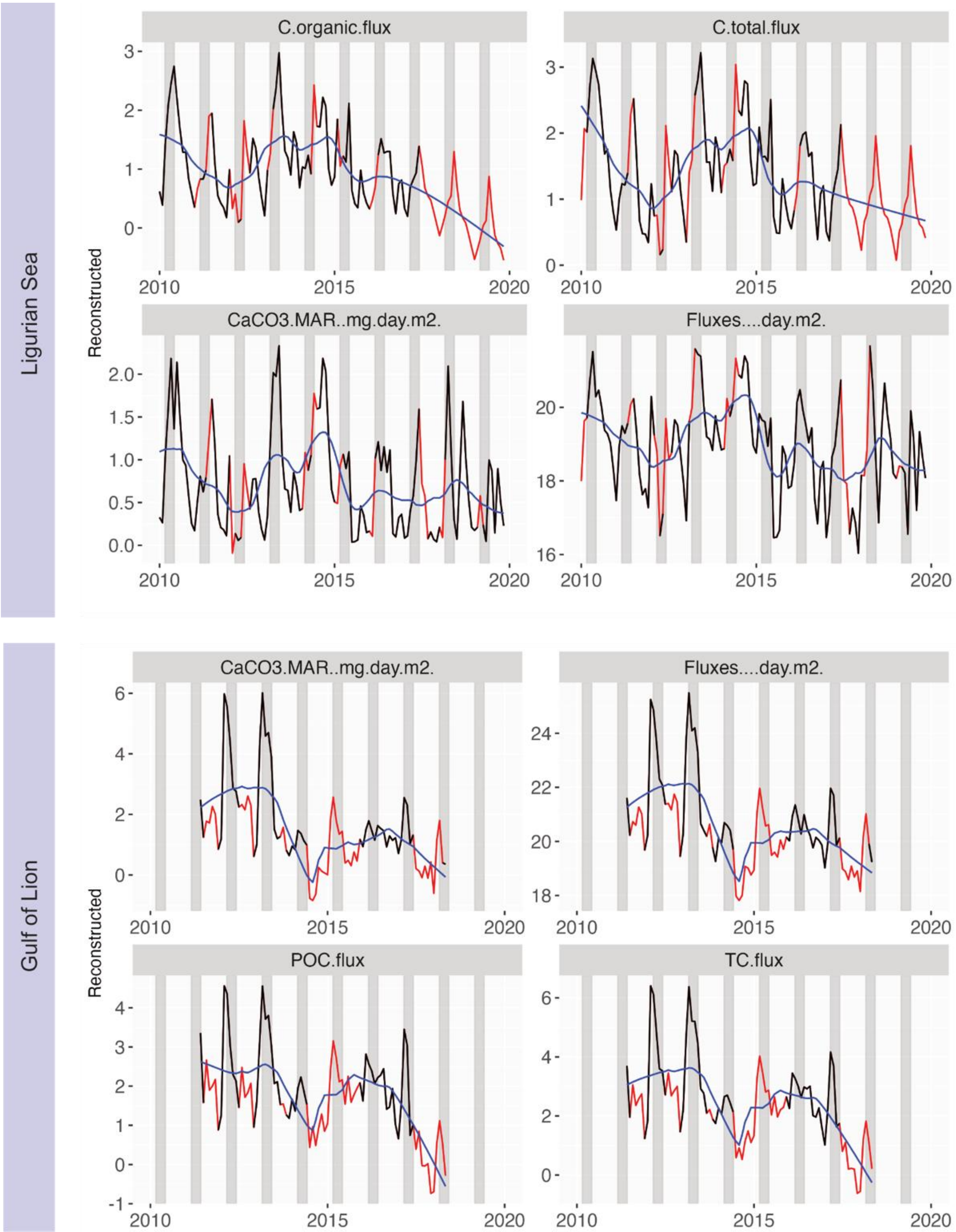

Figure S6 – Interannual fluxes to trap. For each site, values for $CaCO_3$ accumulation rates, total carbon mass fluxes, and total organic carbon are shown (in $mg.m^{-2}.d^{-1}$). Values for total phytoplankton fluxes in $particles.m^{-2}.d^{-1}$ are also shown. All values were logged before analysis. Grey bars represent March, April and May for each year.

3. Species-specific fluxes and relative contributions

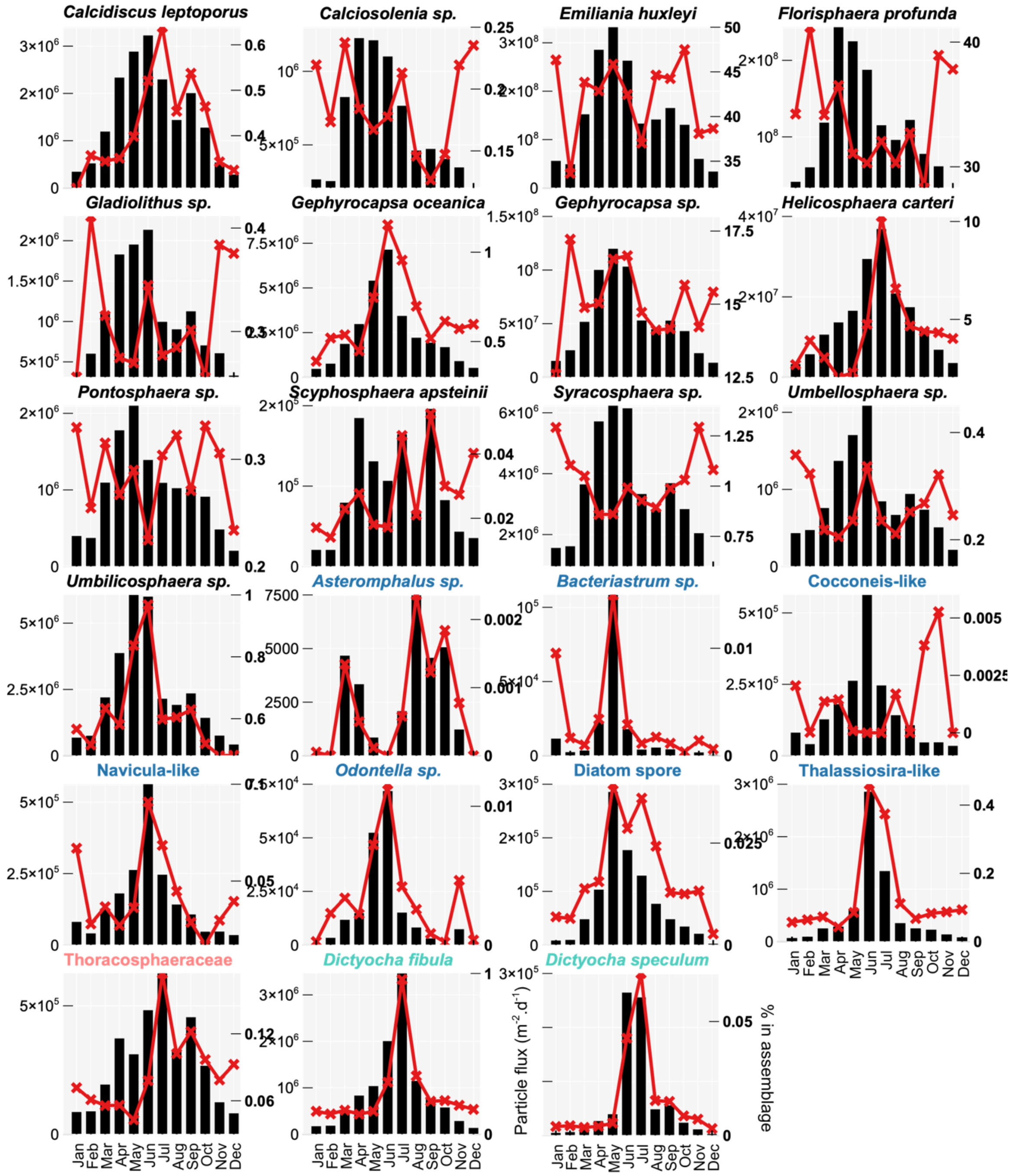

a. Monthly fluxes and relative contributions at DYFAMED

Figure S7 – Species-specific averaged monthly fluxes (in particles.m^{-2}.d^{-1}, left vertical axis, black bars) and relative presence in the assemblage (in %, right vertical axis, red lines) for the DYFAMED sediment trap.

b. Monthly fluxes and relative contributions at Lionceau

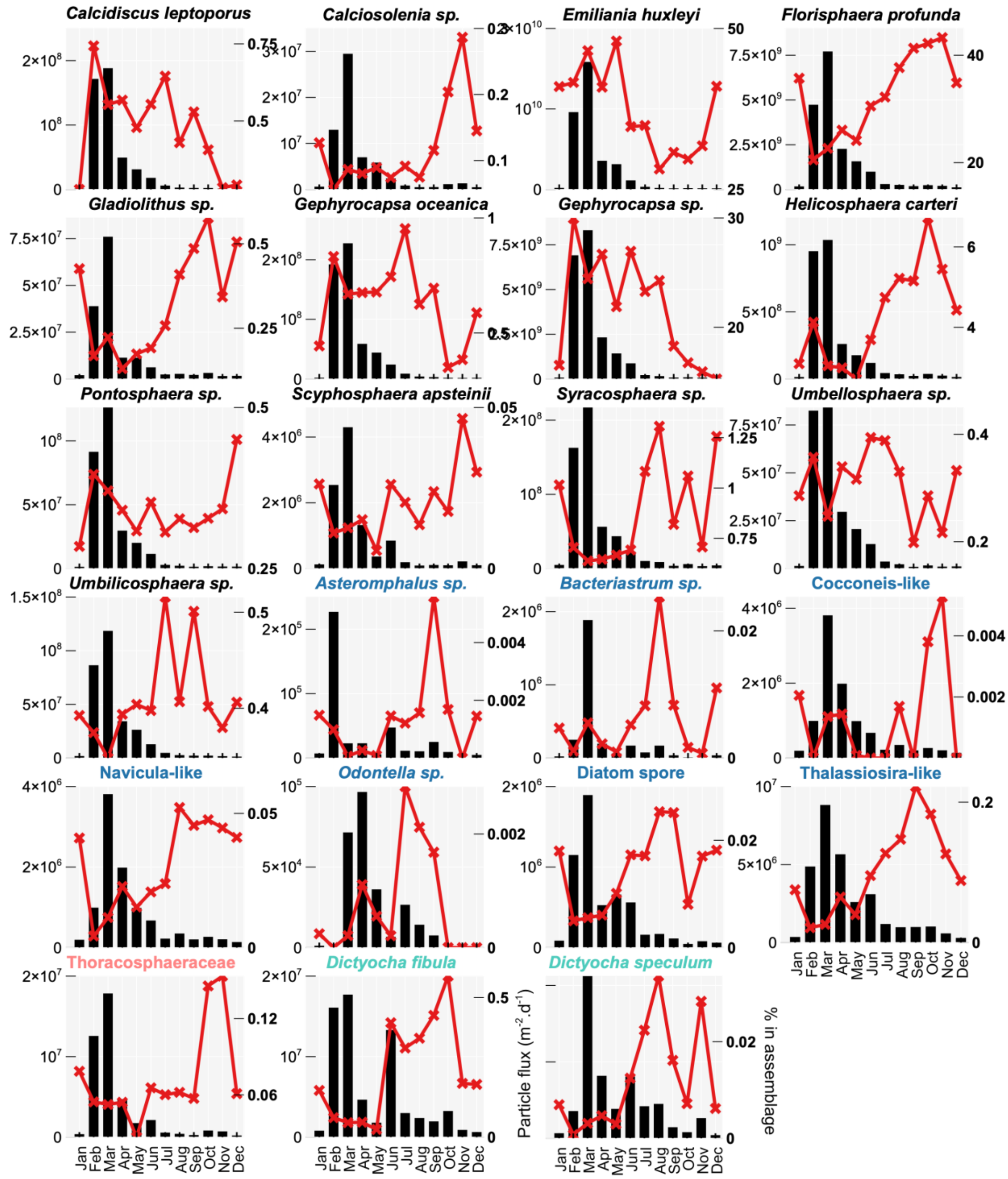

Figure S8 – Species-specific averaged monthly fluxes (in particles.m^{-2}.d^{-1}, left vertical axis, black bars) and relative presence in the assemblage (in %, right vertical axis, red lines) for the Lionceau sediment trap.

c. Interannual fluxes

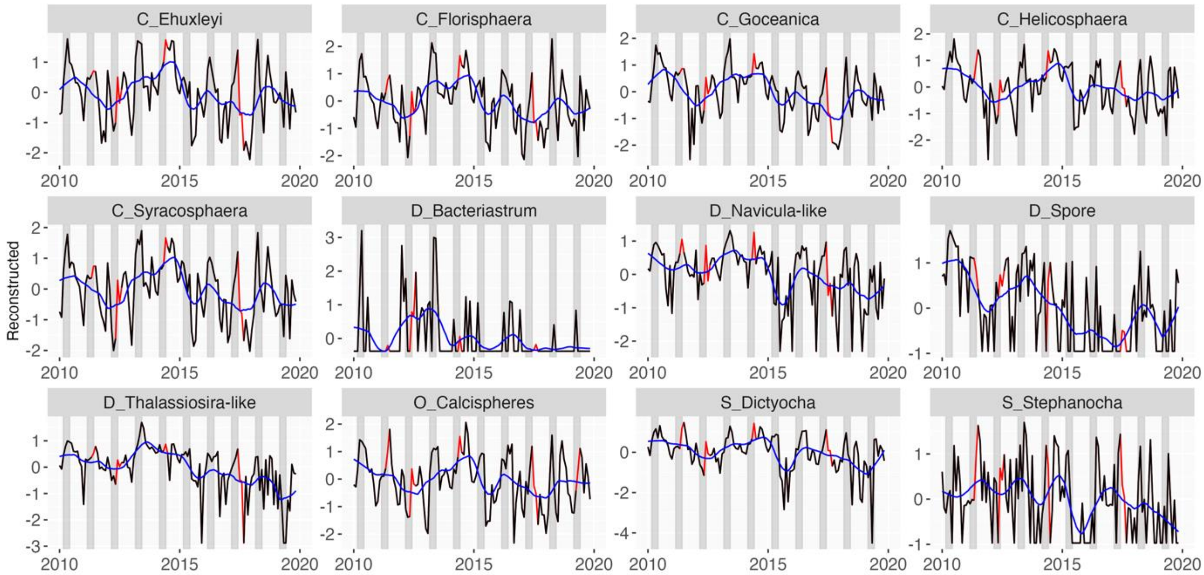

Figure S9 – Species-specific monthly fluxes for the DYFAMED sediment trap for the study period. Fluxes (in particles.$m^{-2}.d^{-1}$) are logged and scaled. Black lines: uninterpreted data. Red lines: reconstructed values using stlplus. Blue lines: trends extracted from the stlplus package. These are the trends used in the PCA analysis. Grey bars represent March, April and May for each year.

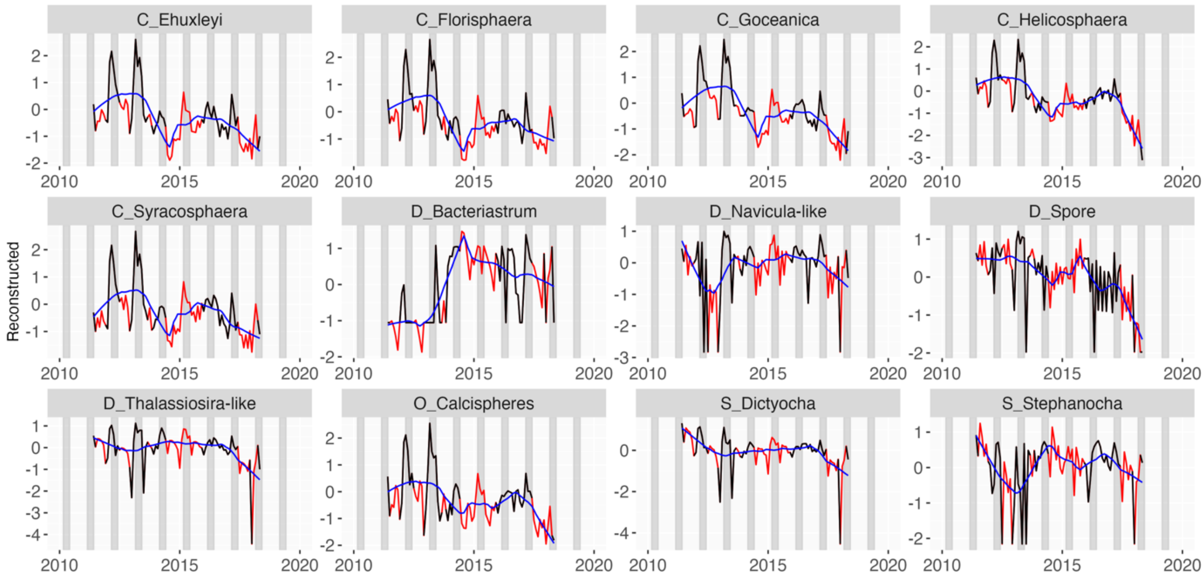

Figure S10 – Species-specific monthly fluxes for the Lionceau sediment trap for the study period. Fluxes (in particles.$m^{-2}.d^{-1}$) are logged and scaled. Black lines: uninterpreted data. Red lines: reconstructed values using stlplus. Blue lines: trends extracted from the stlplus package. These are the trends used in the PCA analysis. Grey bars represent March, April and May for each year.

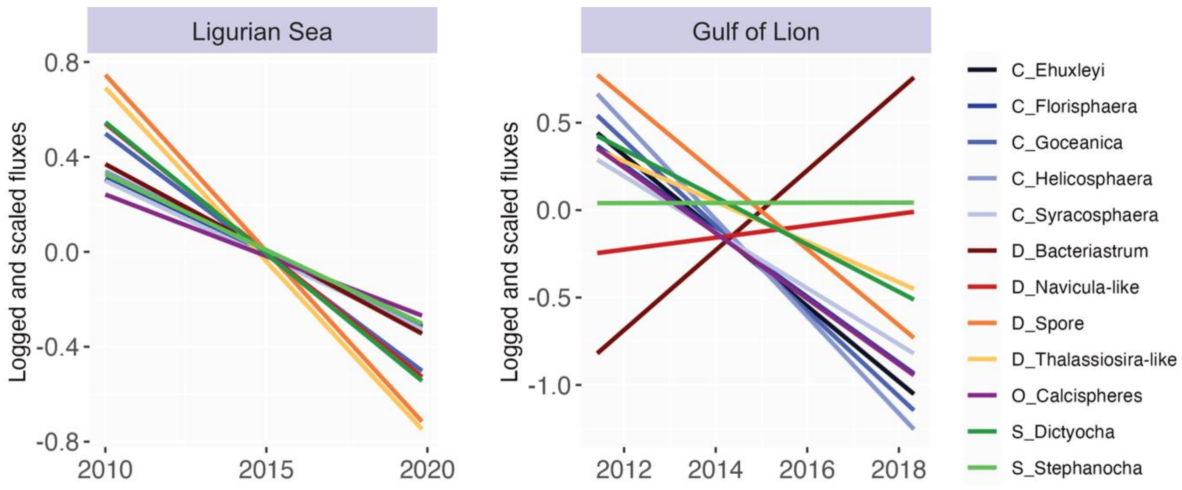

Figure S11 – General trends in fluxes (logged and scaled, expressed in particles.m^{-2}.d^{-1}) at both sites.

4. *Species-specific size variations*

a. DYFAMED interannual variations in size per morphospecies

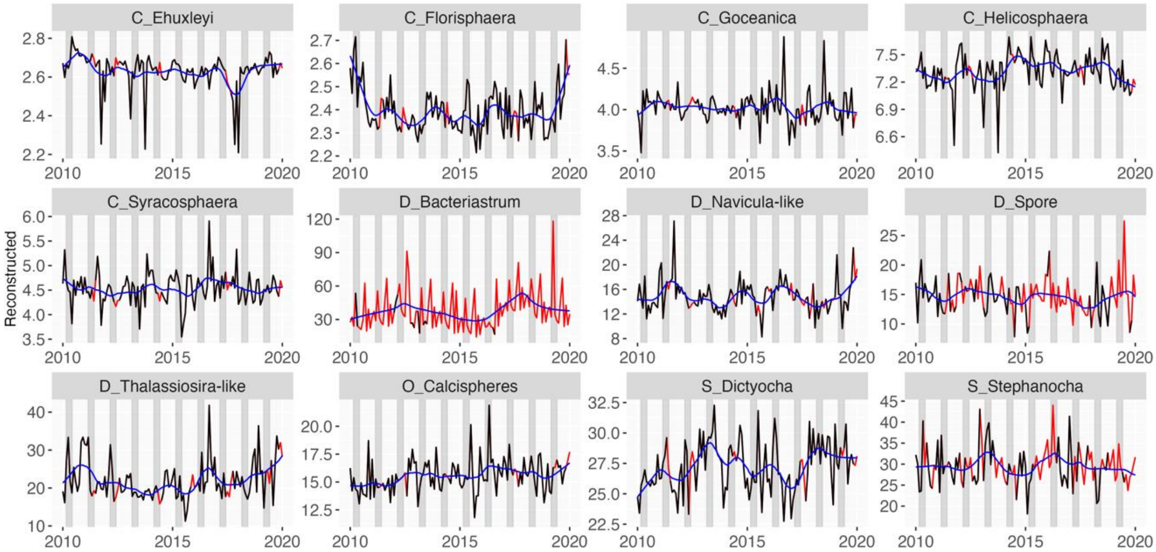

Figure S12 – Species-specific evolution of the mean size (in micrometers) across the period of study for the DYFAMED sediment trap. Black lines: uninterpreted data. Red lines: reconstructed values using stlplus. Blue lines: trends extracted from the stlplus package. Grey bars represent March, April and May for each year.

b. Lionceau interannual variations in size per morphospecies

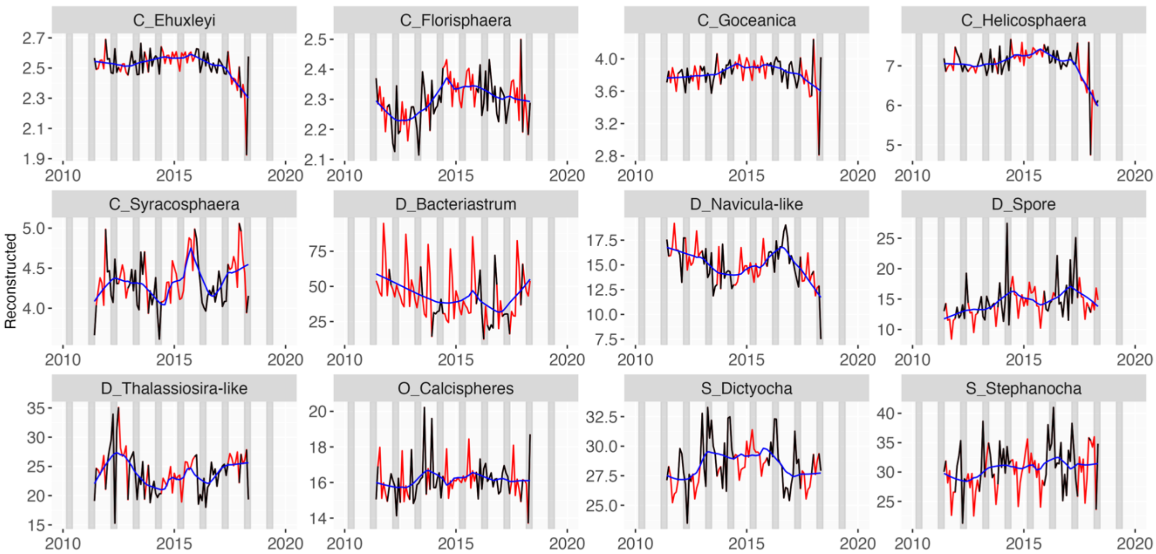

Figure S13 – Species-specific evolution of the mean size (in micrometers) across the period of study for the Lionceau sediment trap. Black lines: uninterpreted data. Red lines: reconstructed values using stlplus. Blue lines: trends extracted from the stlplus package. Grey bars represent March, April and May for each year.

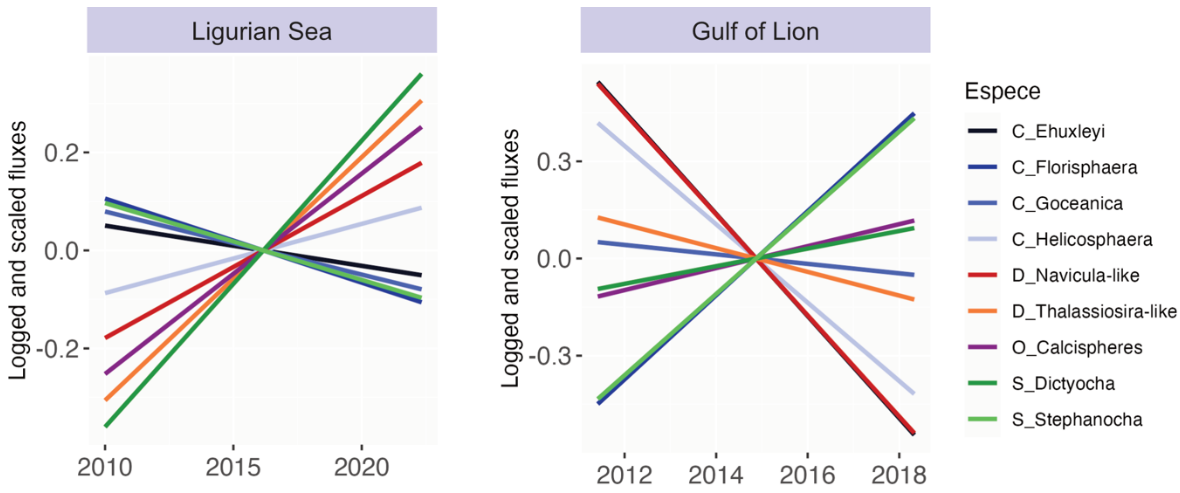

Figure S14 – Trends in size over the period of study. The measurements, in micrometers, were logged and scaled.

Bibliography for supplementary material

Beaufort, L., Gally, Y., Suchéras-marx, B., Ferrand, P., & Duboisset, J. (2020). *Technical Note: A universal method for measuring the thickness of microscopic calcite crystals, based on Bidirectional Circular Polarization*. https://doi.org/10.5194/bg-2020-28

Yang, T., & Wei, K. (2003). How many coccoliths are there in a coccosphere of the extant coccolithophorids? A compilation. *Journal of Nannoplankton Research*, *25*(1), 7–15. https://doi.org/10.58998/jnr2275